Aerosol hygroscopicity over the South-East Atlantic Ocean during the biomass burning season: Part I – From the perspective of scattering enhancement

Lu Zhang[1,2], Michal Segal-Rozenhaimer[1,3,4*], Haochi Che[2*], Caroline Dang[3,4], Junying Sun[5], Ye Kuang[6,7], Paola Formenti[8], Steven G. Howell[9]

[1]Department of Geophysics, Porter School of the Environment and Earth Sciences, Tel Aviv University, Tel Aviv, Israel

[2]Department of Geosciences, University of Oslo, Oslo, Norway

[3]Bay Area Environmental Research Institute, Moffett Field, California, USA

[4]NASA Ames Research Center, Moffett Field, California, USA

[5]State Key Laboratory of Severe Weather & Key Laboratory of Atmospheric Chemistry, Chinese Academy of Meteorological Sciences, Beijing, China

[6]Institute for Environmental and Climate Research, Jinan University, Guangzhou, China

[7]Guangdong-Hongkong-Macau Joint Laboratory of Collaborative Innovation for Environmental Quality, Guangzhou, China

[8]Université Paris Cité and Univ Paris Est Creteil, CNRS, LISA, Paris, France

[9]Department of Oceanography, University of Hawai'i at Mānoa, Honolulu, USA

Correspondence: Michal Segal-Rozenhaimer (msegalro@tauex.tau.ac.il) and Haochi Che (haochi.che@geo.uio.no)

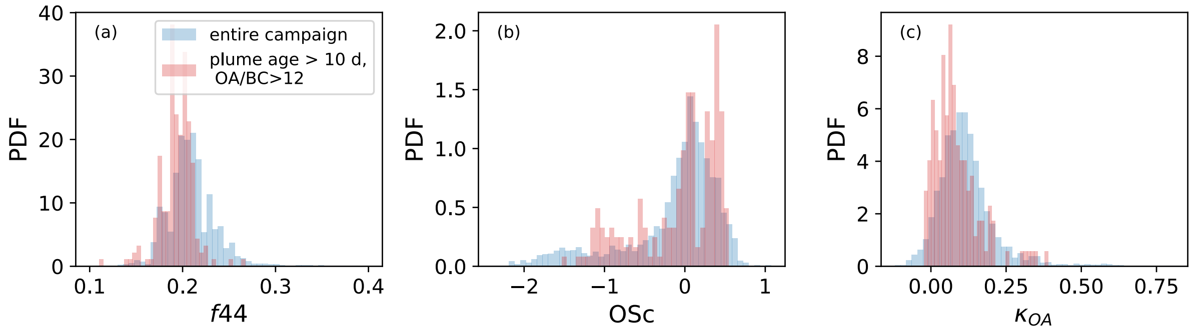

Figure S1. PDF of *f*44, OSc, and κ_{OA} for the entire 2016 and 2018 ORACLES campaign and for aerosols with plume age > 10 days and OA/BC>12.

S1. Sensitivity of *f*(RH) to PNSD

The γ(Fo,κ_{OA},BCr) parameterization was obtained assuming mean PNSD with the geometric mean diameter D_{gn}=150 nm and standard deviation σ_{sg}=1.6. To evaluate the sensitivity of *f*(RH) to PNSD and explore its applicability to broader regions, we calculated the γ with various D_{gn} and σ_{sg} and compared it to those with the mean PNSD. Results are shown in Fig. S2 taking measurements in ORACLES 2018 as an example. The deviations of γ calculated with D_{gn} and σ_{sg} in their interquartile ranges and the 10^{th} - 90^{th} percentile ranges are both smaller than 2% and 3%, respectively, indicating a minor influence of PNSD to γ(Fo,κ_{OA},BCr) parameterization and supporting the application of γ(Fo,κ_{OA},BCr) parameterization to ORACLES 2018. For a broader aerosol population, the deviation is found to be less than 5% when D_{gn} varies from 75 nm to 210 nm (approx. -50% to 35% deviated from the mean D_{gn}) and smaller than 10% with σ_{sg} varying from 1.25 to 1.9 (approx. ±20% deviated from the mean σ_{sg}). The broad ranges of D_{gn} and σ_{sg} suggest that the γ(Fo,κ_{OA},BCr) parameterization can be applied to broader aerosol populations (Hussein et al., 2004; Shen et al., 2015). Cautions are needed when Aitken mode aerosols are dominant such as new particle formation events, as the deviation of γ increases sharply for D_{gn} smaller than 75 nm or σ_{sg} less than 1.25 (Fig. S1). We believe this parameterization would benefit investigations of aerosol direct radiative forcing, aerosol liquid water content, comparison and evaluation of remote sensing and in situ measurements, and visibility degradation.

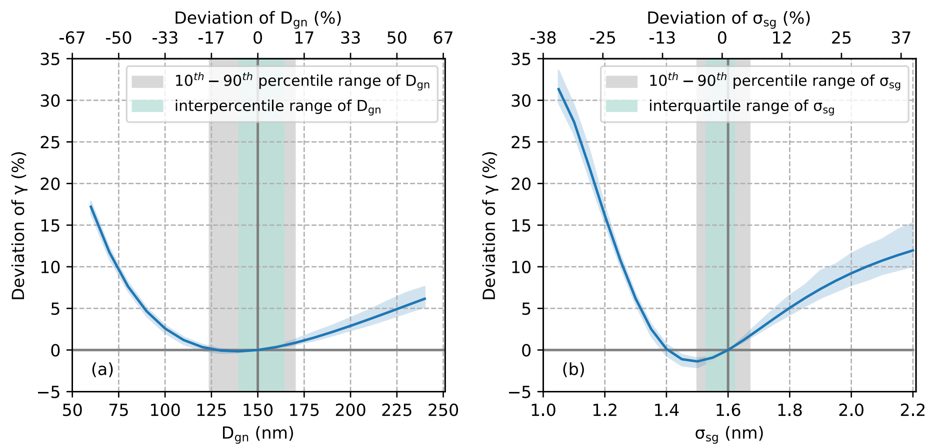

Figure S2. The sensitivity of γ to PNSD. (a) Deviation of γ predicted with various geometric mean diameters D_{gn} to that with the mean D_{gn} in ORACLES 2018 and (b) deviation of γ predicted with various standard deviation σ_{sg} to that with the mean σ_{sg} in ORACLES 2018. Blue lines represent the mean value, and the blue shaded areas represent the 99.7% confidence interval (mean±3 standard deviation). The green and grey shaded areas represent the 25th to 75th percentile and the 10th to 90th percentile of D_{gn} or σ_{sg}, respectively, in ORACLES 2018. The upper x-axis shows the deviation of D_{gn} or σ_{sg} to its mean values in ORACLES 2018.

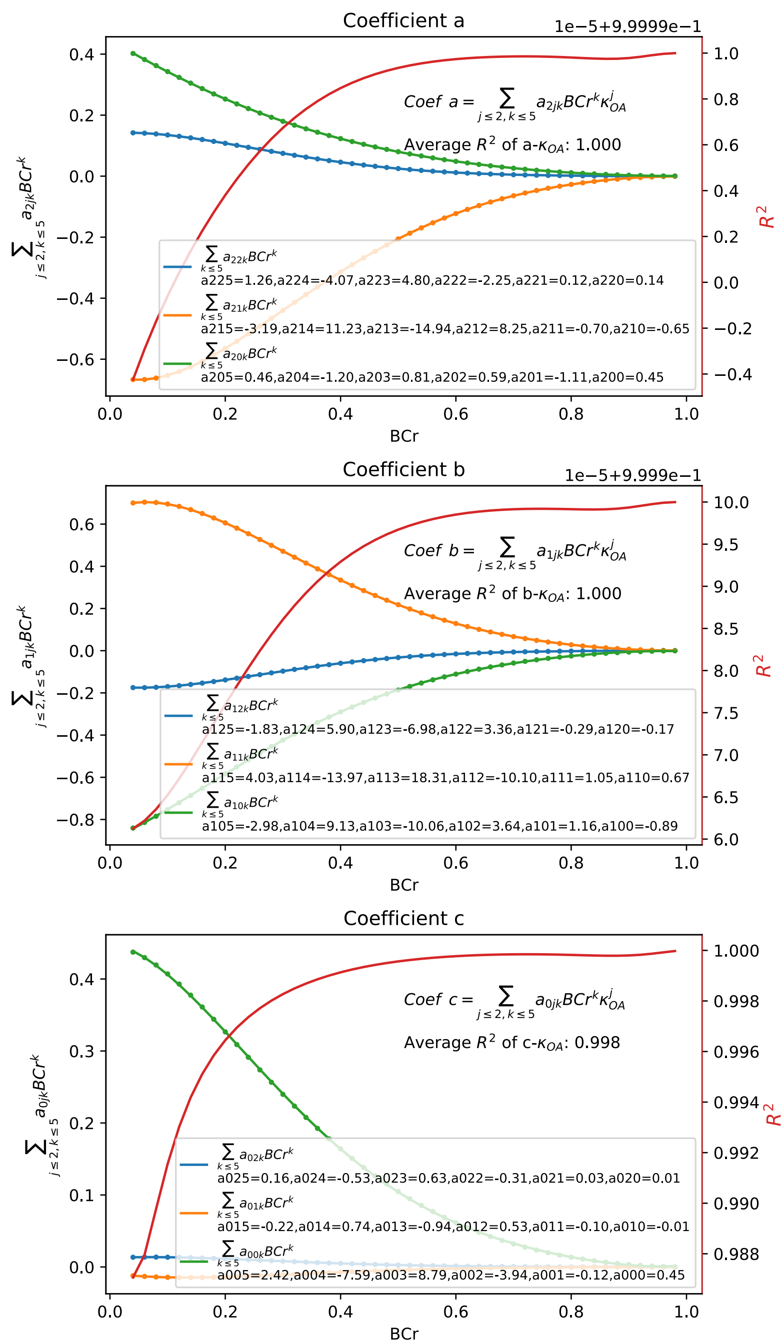

Figure S3. Coefficients a, b, and c of the second-order polynomial fit M(Fo,κ_{OA},BCr) = aFo^2+bFo+c. The a, b, and c can be further fitted into a second-order polynomial fit of κ_{OA} with coefficients being $\sum_{j\le2, k\le5} a_{2jk}BCr^k$, $\sum_{j\le2, k\le5} a_{1jk}BCr^k$, and $\sum_{j\le2, k\le5} a_{0jk}BCr^k$, respectively. Red lines represent the correlation coefficient R^2 of the quadratic relationship between a, b, and c with κ_{OA}

under each BCr, average values are shown in the texts. These coefficients are fitted into a fifth-order polynomial equation with BCr with coefficients shown in each legend.

Table S1. Density (ρ), refractive index ($m=n+ik$) at 540 nm, and hygroscopicity parameter (κ) of inorganics, OA, and BC used in this study.

	$(NH_4)_2SO_4$	NH_4HSO_4	NH_4NO_3	KCl	OA	BC
ρ (g cm^{-3})	1.77(Lide, 2008)	1.78(Lide, 2008)	1.72(Lide, 2008)	1.98(Kuang et al., 2021)	1.4(Alfarra et al., 2006)	1.8(Bond and Bergstrom, 2006; Liu et al., 2017)
$m=n+ik$	1.45[a]	1.44[a]	1.56[a]	1.46[a]	1.65(Feng et al., 2013)	1.95+0.79i(Bond and Bergstrom, 2006; Liu et al., 2021)
κ	0.47(Topping et al., 2005; Gysel et al., 2007; Kim et al., 2020)	0.56(Kuang et al., 2021)	0.58(Topping et al., 2005; Gysel et al., 2007; Kim et al., 2020)	0.89(Kuang et al., 2021)	n/a[b]	0(Kuang et al., 2021; Topping et al., 2005; Gysel et al., 2007)

[a] Aerosol Refractive Index Archive from http://eodg.atm.ox.ac.uk/ARIA/ based on Cotterell et al. (Cotterell et al., 2017) and Querry (Querry, 1985); [b] k_{OA} is determined in the study.

Table S2. The mean and standard deviation of aerosol hygroscopicity related parameters.

	2016		2018	
	>2 km	<2 km	>2 km	<2 km
f(80%)	1.41±0.18	1.51±0.23	1.38±0.15	1.50±0.15
$\kappa_{f(\mathrm{RH})}$	0.22±0.07	0.23±0.09	0.18±0.07	0.21±0.06
κ_{OA}	0.11±0.09	0.14±0.11	0.10±0.06	0.15±0.05
SO4(%)	10.0±2.9	19.7±9.3	13.3±3.7	18.9±5.4
OA(%)	67.5±5.9	60.1±9.6	65.7±4.0	51.6±9.2
Age (d)	7.2±2.6	8.6±1.8	6.3±1.2	9.3±1.4
*f*44	0.21±0.03	0.22±0.03	0.21±0.02	0.24±0.03

Table S3. Parameterization coefficients of M(Fo,κ_{OA},BCr) and γ(Fo,κ_{OA}=0,BCr) in Eq. 4 and 5. Columns are the subscripts of parameter a. a_{X5} with X of 00 represents a_{005} (*i*=0, *j*=0, *k*=5) used in Eq. 5.

Subscript X	a_{X5}	a_{X4}	a_{X3}	a_{X2}	a_{X1}	a_{X0}
00	2.42	-7.59	8.79	-3.94	-0.12	0.45
01	-0.22	0.74	-0.94	0.53	-0.10	-0.01
02	0.16	-0.53	0.63	-0.31	0.03	0.01
10	-2.98	9.13	-10.06	3.64	1.16	-0.89

11	4.03	-13.97	18.31	-10.10	1.05	0.67
12	-1.83	5.90	-6.98	3.36	-0.29	-0.17
20	0.46	-1.20	0.81	0.59	-1.11	0.45
21	-3.19	11.23	-14.94	8.25	-0.70	-0.65
22	1.26	-4.07	4.80	-2.25	0.12	0.14
0	0.83	-3.13	4.44	-2.66	-0.14	0.67
1	0.61	-1.94	2.56	-1.90	1.33	-0.66
2	-1.25	4.48	-6.31	4.21	-1.13	-0.00

$$M(Fo, \kappa_{OA}, BCr) = \begin{bmatrix} Fo^2 & Fo & 1 \end{bmatrix} \begin{bmatrix} \begin{bmatrix} {\kappa_{OA}}^2 & \kappa_{OA} & 1 \end{bmatrix} \left(\begin{bmatrix} a_{225} & a_{224} & a_{223} & a_{222} & a_{221} & a_{220} \\ a_{215} & a_{214} & a_{213} & a_{212} & a_{211} & a_{210} \\ a_{205} & a_{204} & a_{203} & a_{202} & a_{201} & a_{200} \end{bmatrix} \begin{bmatrix} BCr^5 \\ BCr^4 \\ BCr^3 \\ BCr^2 \\ BCr \\ 1 \end{bmatrix} \right) \\ \begin{bmatrix} {\kappa_{OA}}^2 & \kappa_{OA} & 1 \end{bmatrix} \left(\begin{bmatrix} a_{125} & a_{124} & a_{123} & a_{122} & a_{121} & a_{120} \\ a_{115} & a_{114} & a_{113} & a_{112} & a_{111} & a_{110} \\ a_{105} & a_{104} & a_{103} & a_{102} & a_{101} & a_{100} \end{bmatrix} \begin{bmatrix} BCr^5 \\ BCr^4 \\ BCr^3 \\ BCr^2 \\ BCr \\ 1 \end{bmatrix} \right) \\ \begin{bmatrix} {\kappa_{OA}}^2 & \kappa_{OA} & 1 \end{bmatrix} \left(\begin{bmatrix} a_{025} & a_{024} & a_{023} & a_{022} & a_{021} & a_{020} \\ a_{015} & a_{014} & a_{013} & a_{012} & a_{011} & a_{010} \\ a_{005} & a_{004} & a_{003} & a_{002} & a_{001} & a_{000} \end{bmatrix} \begin{bmatrix} BCr^5 \\ BCr^4 \\ BCr^3 \\ BCr^2 \\ BCr \\ 1 \end{bmatrix} \right) \end{bmatrix} \quad \text{(S1)}$$

$$\gamma(Fo, \kappa_{OA} = 0, BCr) = \begin{bmatrix} Fo^2 & Fo & 1 \end{bmatrix} \left(\begin{bmatrix} a_{25} & a_{24} & a_{23} & a_{22} & a_{21} & a_{20} \\ a_{15} & a_{14} & a_{13} & a_{12} & a_{11} & a_{10} \\ a_{05} & a_{04} & a_{03} & a_{02} & a_{01} & a_{00} \end{bmatrix} \begin{bmatrix} BCr^5 \\ BCr^4 \\ BCr^3 \\ BCr^2 \\ BCr \\ 1 \end{bmatrix} \right) \tag{S2}$$

References

Alfarra, M. R., Paulsen, D., Gysel, M., Garforth, A. A., Dommen, J., Prévôt, A. S. H., Worsnop, D. R., Baltensperger, U., and Coe, H.: A mass spectrometric study of secondary organic aerosols formed from the photooxidation of anthropogenic and biogenic precursors in a reaction chamber, Atmospheric Chem. Phys., 6, 5279–5293, https://doi.org/10.5194/acp-6-5279-2006, 2006.

Bond, T. C. and Bergstrom, R. W.: Light Absorption by Carbonaceous Particles: An Investigative Review, Aerosol Sci. Technol., 40, 27–67, https://doi.org/10.1080/02786820500421521, 2006.

Cotterell, M. I., Willoughby, R. E., Bzdek, B. R., Orr-Ewing, A. J., and Reid, J. P.: A complete parameterisation of the relative humidity and wavelength dependence of the refractive index of hygroscopic inorganic aerosol particles, Atmospheric Chem. Phys., 17, 9837–9851, https://doi.org/10.5194/acp-17-9837-2017, 2017.

Feng, Y., Ramanathan, V., and Kotamarthi, V. R.: Brown carbon: a significant atmospheric absorber of solar radiation?, Atmospheric Chem. Phys., 13, 8607–8621, https://doi.org/10.5194/acp-13-8607-2013, 2013.

Gysel, M., Crosier, J., Topping, D. O., Whitehead, J. D., Bower, K. N., Cubison, M. J., Williams, P. I., Flynn, M. J., McFiggans, G. B., and Coe, H.: Closure study between chemical composition and hygroscopic growth of aerosol particles during TORCH2, Atmospheric Chem. Phys., 7, 6131–6144, https://doi.org/10.5194/acp-7-6131-2007, 2007.

Hussein, T., Puustinen, A., Aalto, P. P., Mäkelä, J. M., Hämeri, K., and Kulmala, M.: Urban aerosol number size distributions, Atmospheric Chem. Phys., 4, 391–411, https://doi.org/10.5194/acp-4-391-2004, 2004.

Kim, N., Yum, S. S., Park, M., Park, J. S., Shin, H. J., and Ahn, J. Y.: Hygroscopicity of urban aerosols and its link to size-resolved chemical composition during spring and summer in Seoul, Korea, Atmospheric Chem. Phys., 20, 11245–11262, https://doi.org/10.5194/acp-20-11245-2020, 2020.

Kuang, Y., Huang, S., Xue, B., Luo, B., Song, Q., Chen, W., Hu, W., Li, W., Zhao, P., Cai, M., Peng, Y., Qi, J., Li, T., Wang, S., Chen, D., Yue, D., Yuan, B., and Shao, M.: Contrasting effects of secondary organic aerosol formations on organic aerosol hygroscopicity, Atmospheric Chem. Phys., 21, 10375–10391, https://doi.org/10.5194/acp-21-10375-2021, 2021.

Lide, D. R. (Ed.): CRC Handbook of Chemistry and Physics, 89th Edition, 89th edition., CRC Press, Boca Raton, 2736 pp., 2008.

Liu, D., Whitehead, J., Alfarra, M. R., Reyes-Villegas, E., Spracklen, D. V., Reddington, C. L., Kong, S., Williams, P. I., Ting, Y.-C., Haslett, S., Taylor, J. W., Flynn, M. J., Morgan, W. T., McFiggans, G., Coe, H., and Allan, J. D.: Black-carbon absorption enhancement in the atmosphere determined by particle mixing state, Nat. Geosci., 10, 184–188, https://doi.org/10.1038/ngeo2901, 2017.

Liu, D., Li, S., Hu, D., Kong, S., Cheng, Y., Wu, Y., Ding, S., Hu, K., Zheng, S., Yan, Q., Zheng, H., Zhao, D., Tian, P., Ye, J., Huang, M., and Ding, D.: Evolution of Aerosol Optical Properties from Wood Smoke in Real Atmosphere Influenced by Burning Phase and Solar Radiation, Environ. Sci. Technol., 55, 5677–5688, https://doi.org/10.1021/acs.est.0c07569, 2021.

Querry, M. R.: Optical Constants, US Army Chem. Res., Aberdeen Proving Ground, 418, 1985.

Shen, X. J., Sun, J. Y., Zhang, X. Y., Zhang, Y. M., Zhang, L., Che, H. C., Ma, Q. L., Yu, X. M., Yue, Y., and Zhang, Y. W.: Characterization of submicron aerosols and effect on visibility during a severe haze-fog episode in Yangtze River Delta, China, Atmos. Environ., 120, 307–316, https://doi.org/10.1016/j.atmosenv.2015.09.011, 2015.

Topping, D. O., McFiggans, G. B., and Coe, H.: A curved multi-component aerosol hygroscopicity model framework: Part 1 – Inorganic compounds, Atmospheric Chem. Phys., 5, 1205–1222, https://doi.org/10.5194/acp-5-1205-2005, 2005.